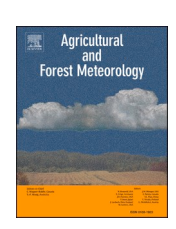
ELSEVIER

Contents lists available at ScienceDirect

Agricultural and Forest Meteorology

journal homepage: www.elsevier.com/locate/agrformet





Canopy wetting patterns and the determinants of dry season dewfall in an old growth Douglas-fir canopy

Adam Sibley a, a, Mark Schulze a, Julia Jones b, Adam Kennedy a, Christopher Still a

- ^a The Department of Forest Ecosystems and Society, Oregon State University, Corvallis, OR 97331, USA
- ^b The College of Earth, Ocean and Atmospheric Sciences, Oregon State University, Corvallis, OR 97331, USA

ARTICLE INFO

Keywords:
Canopy microclimate
Surface wetting
Rainfall interception
Dew
Dewfall prediction
Frost

ABSTRACT

Canopy wetting and drying has a variety of effects on the function of plant foliage, ranging from increased risk of pathogenic infection to reduced diffusion of gases to enhanced leaf water status in plants capable of foliar water uptake (FWU). Projected shifts in rainfall regimes and increases in summertime vapor pressure deficit will likely change the timing and duration of canopy wetting, yet current patterns of wetting are poorly understood. In this study, we investigated patterns of wetting by source (rain, dew, or frost), at different canopy heights, and at annual, seasonal and diurnal time scales using leaf wetness sensor data collected over a 4-year period in an old growth Douglas-fir tree in a temperate wet forest. We found that canopy layers were wet for roughly half the year with strong seasonal variation, staying wet 83% of the cold winter season but only 1.9% of the dry season. Upper canopy layers experienced higher wetting frequency and shorter wetting duration in all seasons compared to lower canopy layers. Outside of the dry season, wetness was predominantly caused by rain, while in the dry season the predominant source was dewfall. Throughout the year and particularly in the dry season, dewfall was restricted to the upper canopy, occurring on 28.5% of dry season nights. Multiple models which use meteorological variables to predict dewfall timing and length were developed and evaluated. Using in-tree observations, dry season dewfall was best predicted with a logistic model using dewpoint depression as a predictor. Using observations from a nearby weather station in a clearing, dry season dewfall was best predicted with the Penman equation, a biophysical model. The most important determinant of dry season dewfall in our study was sufficient nighttime cooling of the air, suggesting that increasing nighttime temperatures will lead to a decrease in dew formation frequency in the future.

1. Introduction

While changes in climate are evident at regional and continental scales, it is the propagation of these changes through the microclimates of terrestrial ecosystems that will determine species responses and changes in ecological interactions (Davis et al., 2019; De Frenne et al., 2013; Pincebourde and Casas, 2015; Storlie et al., 2014). Episodes of canopy wetting and drying are an important determinant of forest microclimate conditions. When surface water evaporates, it significantly increases the latent heat flux component of the canopy energy balance (Pypker et al., 2017) and helps moderate fluctuations in air temperature, while also humidifying the canopy boundary layer and increasing the water use efficiency of plants (Meinzer et al., 1997). Surface wetness has a variety of direct impacts on vegetation as well. In moist forests like

those of the U.S. Pacific Northwest (PNW), patterns of surface wetting and drying determine niche suitability for poikilohydric epiphytes such as bryophytes and lichens, which in turn play important roles in forest nutrient cycling (Johnson et al., 1982). Tree species across a diversity of forest types experience both beneficial and harmful effects related to foliar wetting (Dawson and Goldsmith, 2018), ranging from added hydration via foliar water uptake to increased rates of infection by pathogens as leaves stay wet longer (Berry et al., 2018). Foliar water uptake has demonstrated importance for a wide variety of tree species, including tall tree species where upper foliage experiences perennially low water potentials (Limm et al., 2009), species exposed to seasonal dry periods (Binks et al., 2019), and species in ecosystems where dew or fog water make up a significant portion of the water balance (Fischer et al., 2016).

^{*} Corresponding author.

E-mail address: adam.sibley@oregonstate.edu (A. Sibley).

¹ Present address: 321 Richardson Hall, 3180 SW Jefferson way, Corvallis, OR, 97370.

Despite the importance of surface wetting to forest microclimate and tree health, efforts to model spatial and temporal patterns of wetting and drying have yielded inconsistent results (Greve et al., 2014) and relatively few studies have addressed it directly (Ritter et al., 2019; Binks et al., 2021), because of the difficulty of upper canopy access and the sparsity of observations. The majority of past studies using leaf wetness sensors have been short in duration (Aparecido et al., 2016; Dietz et al., 2007; Letts and Mulligan, 2005; Klemm et al., 2002) and many focus on agricultural crops, not natural forests (Bassimba et al., 2017; Schmitz and Grant, 2009; Sentelhas et al., 2005). Efforts to model vertical variation in microclimate conditions have also been confounded by the 3-D complexity of canopy structures, a complexity which tends to increase with forest age commensurate with increases in overall Leaf Area Index (LAI) (Ehbrecht et al., 2017; von Arx et al., 2013), increased epiphyte density (McCune, 1993), greater tree height, and increased horizontal heterogeneity due to tree fall. Absent an ability to accurately predict vertical variations in microclimate, predicting differences in drying times after rain events or the formation of dew or frost on different canopy layers is intractable. In addition to the confounding effects of structural complexity, seasonal changes in weather patterns may greatly change the frequency of rain events, local cycling of water, and evaporative demand throughout the year. Owing to these challenges, little is known about the vertical patterns of wetting and drying within forests and how they vary on interannual and seasonal timescales.

In this study we directly observed surface wetting and microclimate conditions throughout the canopy of a 65 m tall old-growth Douglas-fir tree at the H.J. Andrews Experimental Forest in the Oregon Cascade Range. Using a 4-year record of in-tree observations along with fifteen years of observations from a nearby weather station in a clearing, we asked how frost, rain wetting, and dew wetting varied on inter-annual and seasonal timescales. We also assessed the accuracy of two different models for predicting dry season dewfall. In the first instance, we tested the accuracy of Penman equation predictions using in-tree data and data from a climate station in a nearby clearing, as this is a common technique used to predict dew occurrence when direct observations are not available (Monteith and Unsworth, 2013; Andrade, 2003). In the second, we tested the accuracy of logistic models trained on in-tree measurements to identify the most parsimonious set of measurements that reliably capture dew events, with the aim of informing future efforts of instrumenting canopies at a broader spatial scale. We further interrogated the conditions under which dry season dewfall occurred in order to better understand the factors that influence this important subsidy of water to canopy foliage and how it may be affected by future change.

2. Methods

2.1. Site description

Data for this study were collected at the H.J. Andrews Experimental Forest (henceforth Andrews Forest) in Blue River, OR (Fig. 1). The research forest is a 6400-hectare parcel containing deep valleys separated from ridge tops by steep slopes. Elevations range from 430 to 1630 m. Soils are volcanic in origin (Swanson and James, 1975) and range in texture from gravelly clay loam in alluvial areas to gravelly sandy loam and bedrock talus at higher elevations (Rothacher et al., 1967). The forest is composed of a mixture of plantation and old growth conifer stands. Douglas-fir (Pseudotsuga menziesii (Mirb.) Franco) is the dominant tree species in plantations and is a canopy dominant in lower elevation old growth patches along with western redcedar (Thuja plicata Donn ex. D Don) and western hemlock (Tsuga heterophylla (Raf.) Sarg.). Mean annual precipitation is 2077 mm (S.D. 477 mm) and mean annual temperature is 9.1 $^{\circ}\text{C}$ (S.D. 0.86 $^{\circ}\text{C}),$ as measured over the past 30 years at the Primary Meteorological Station (see Section 2.2). The synoptic climate regime is Mediterranean - winters are cool and rainy while summers are warm and relatively rain-free, with shoulder seasons that

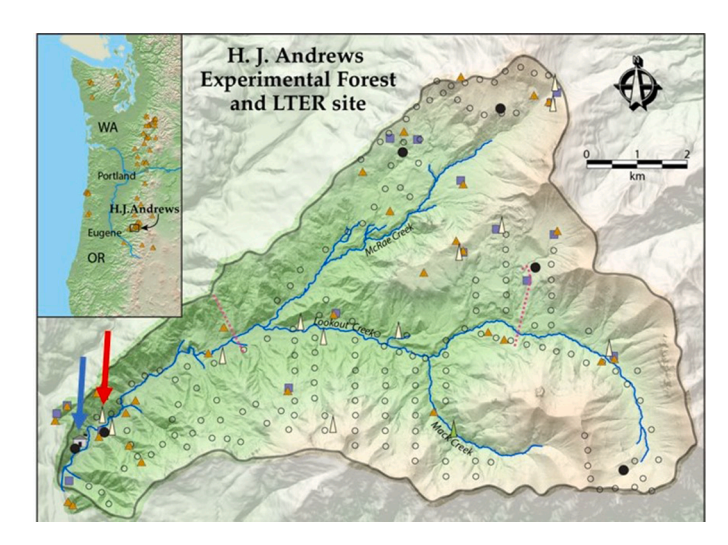


Fig. 1. Map of the H.J. Andrews Experimental Forest, with the position of the instrumented tree (Discovery Tree) marked with a red arrow. The blue arrow indicates the location of the meteorological station where net radiation and precipitation were measured.

include a combination of dry and wet spells. This rainfall seasonality makes it instructive to discuss annual statistics in this study in terms of a water year, which runs from the start of fall to the start of the subsequent fall. Mean rainfall totals for the winter months of December, January and February are 8.5 times greater than in June, July and August, while potential evapotranspiration (PET) is 7 times lower for those same periods (868.0 mm vs. 101.7 mm rainfall, 83.9 mm vs. 593.4 mm PET) across the years where net radiation data is available (2013–2019). While these statistics give some sense of the strength of seasonality in the moisture balance, using seasonal boundaries based on calendar months can mask significant interannual variability in dry season timing and so we developed an empirical routine for finding seasonal boundaries (see Section 2.4).

2.2. Meteorological measurements

Meteorological observations were made in two locations - along the vertical axis of an old growth Douglas-fir tree and in a nearby open meadow. The measurement tree, hereafter called the Discovery Tree, is approximately 450 years old, stands 65 m tall, and has a diameter of 122 cm at breast height (Fig. 2). The tree is in a grove of other old growth Douglas-fir, western hemlock and western redcedar trees, and is bordered to the north by a 60-year-old plantation forest. Instrument clusters were installed at 1.5, 10, 20, 30, 40 and 56 m above ground level (a.g.l.) on the north side of the Discovery Tree (Fig. 2b). This study used the following observations from the instrument clusters: air temperature (T_{air}, °C, at all heights), relative humidity (RH, %, 1.5 and 56 m heights), wind speed and direction (m s⁻¹ and degrees, 1.5 and 56 m heights) and leaf wetness (mV, all heights). In cases where R_{net} is needed for calculations using in-tree data at the 56 m observation height, values are taken from the nearby Primary Meterological Station, where the level of sky exposure is broadly similar as is found at the 56 m observation height. All measurements at all heights were recorded at a five-minutes interval and span the calendar years 2017–2020.

The second measurement location in this study was the Primary Meteorological Station (hereafter "PRIMET"), which was established in 1972 and is situated in a small clearing at the bottom of a steep forested hillslope, \sim 700 m southwest of the measurement tree. From PRIMET we used measurements of net radiation (R_{net} , W m $^{-2}$), T_{air} (°C), RH (%), downwelling solar radiation (R_{solar} , W m $^{-2}$), precipitation (P, mm), and volumetric water content at 100 cm depth (VWC, %). For more information on the specific instruments deployed on the Discovery Tree and

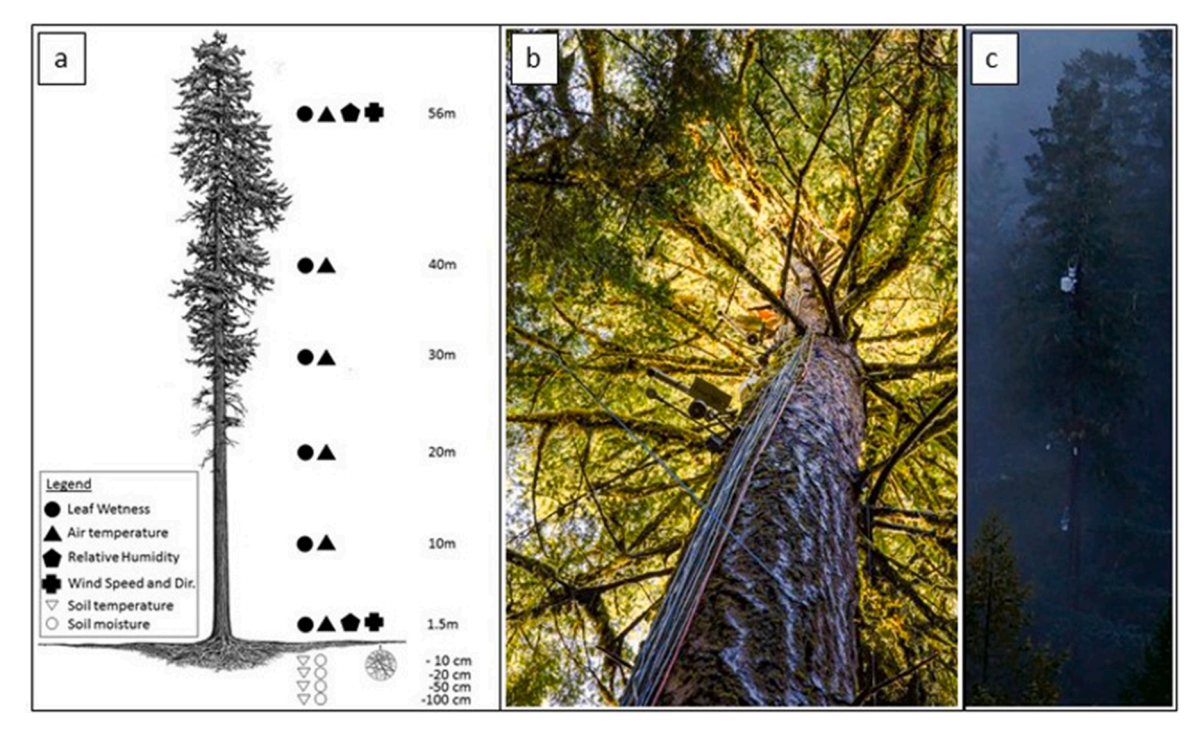


Fig. 2. (a) Illustration of the measurement tree, measurement heights within the tree, and the variables recorded at each height (illustration by Van Pelt and North (1996)). (b) View of the instrument clusters at 20 and 30 m above ground (photo credit Leah Wilson). (c) View of the upper 30 m of the tree. The white instrument enclosure in the photograph is at 56 m a.g.l. (photo credit Adam Sibley).

at PRIMET, as well as the data QA/QC procedure we used, see supplemental material S.1 and Daly et al. (2019). From the basic observations described here, we calculated Potential Evapotranspiration (PET) using the Priestley-Taylor equation (Priestley and Taylor, 1972), latent heat flux (LE) using the Penman equation (Monteith and Unsworth, 2013), and Dewpoint Depression (DPD). For PET:

$$PET = \alpha \frac{\Delta}{\Delta + \gamma} R_{net}$$
 (1)

Where α is 1.26 (an empirical constant), γ is the psychrometric constant (0.066 kPa $^{\circ}$ C $^{-1}$), and Δ is the slope of the saturation vapor pressure curve at a given T_{air} (kPa $^{\circ}$ C $^{-1}$) and is defined as:

$$\Delta = \frac{17.502 \times 240.9 \text{ es}(T_{air})}{(T_{air} + 240.97)^2}$$
 (2)

In the above, $es(T_{air})$ is the saturation vapor pressure and is given by the following, with T_{air} in Celsius:

$$es(T_{air}) = 0.61121exp\left(\frac{17.502 \times T_{air}}{T_{air} + 240.97}\right)$$
(3)

From $\mbox{es}(T_{\mbox{\scriptsize air}})$ and relative humidity (RH), actual vapor pressure is given as:

$$e = \operatorname{es}(T_{air}) * RH \tag{4}$$

From these same quantities, one can calculate both specific humidity (SH) and predict the rate of latent heat flux during periods of minimal transpiration using the Penman equation. For specific humidity:

$$SH = \frac{0.622 * e}{101.3 - (0.378 * e)} \tag{5}$$

For the Penman equation:

$$LE = \frac{\Delta R_{net} + \rho c_p(es(T_{air}) - e)r_H^{-1}}{\Delta + \gamma \binom{r_V}{r_H}}$$
(6)

Where R_{net} is net radiation (W m⁻²), ρ is the density of air (1.15 kg

 m^{-3}), c_p is the specific heat capacity of air (1005 J kg $^{-1}$ C $^{-1}$), the ratio of r_V to r_H is assumed to be constant at 0.926, and r_H – aerodynamic resistance to heat transfer – is given by Campbell and Norman (1998):

$$r_H = 7.4 \sqrt{\frac{d}{u}} \tag{7}$$

Where d is the average of foliage length and width in meters (here 0.03 m and 0.003 m, respectively) and u is wind speed in m s⁻¹. The above formulation of r_H applies to the leaf scale, while in the big-leaf canopy conceptualization of the Penman equation r_H is divided by the LAI of the canopy in question (Bonan, 2008). For both in-canopy measurements and PRIMET measurements it was not obvious whether the leaf-scale or canopy-scale formulation was appropriate, or what the appropriate LAI value might be in the big-leaf canopy formulation. Thus, we conducted a sensitivity test where LAI was allowed to vary across a range of 0.001-16 (LAI = 1 is a de-facto test of the leaf-level formulation) and Penman predictions of dewfall were compared to classified LWS values (Section 2.3, Supplemental S.2). The results of this test indicated that dewfall was best predicted when rH in PRIMET-based predictions was scaled by an LAI of 10, while for in-tree measurements an LAI of 1 was optimal. All presented results for each set of meteorological predictors use these LAI values.

While Eq. (1) can be forced with $R_{\rm net}$ data from the years 2014–2020, net radiation data was not available prior to 2014. For the years 2004–2014, daytime $R_{\rm net}$ was estimated using the following equation, adapted from McMahon et al. (2013):

$$R_{net\ approx} = R_{solar}(1-\alpha) - \sigma T_{air}^4(0.34 - 0.24\sqrt{e}) \left(\frac{1.35 R_{solar}}{R_{stangles} - 0.35}\right)$$
 (8)

Where R_{solar} is incoming shortwave radiation (W m $^{-2}$), α is albedo (0.28 in this study, determined using average ratio of SW_{out} : Sw_{in} when R_{net} is available), σ is the Stefan-Boltzmann constant, T_{air} is in Kelvin, and $R_{clearsky}$ is estimated clear sky incoming shortwave. $R_{clearsky}$ that accounts for topographic shading was modeled as described in Daly et al. (2007) but with a climatological clear-sky optical depth and surface albedo varying by day of year. Dewpoint depression was calculated

as air temperature minus the dewpoint temperature:

$$DPD = T_{air} - \frac{T^*}{1 - A^{-1} \ln\left(\frac{e}{e_s(T^*)}\right)}$$

$$\tag{9}$$

Where A = 19.65, T* is 273 $^{\circ}$ K and $e_s(T^*)$ is 0.611 kPa.

2.3. Wetness measurements

Canopy wetness was measured at each instrument cluster on the Discovery Tree (Fig. 2) at five-minutes intervals using Phytos 31 Leaf wetness sensors (METER group, Pullman, WA). These sensors are fiberglass, leaf-shaped devices 12 cm long and 8.5 cm wide, with a specific heat capacity of 1480 J m⁻² K⁻¹. Measurements are made by applying an excitation voltage to electrodes embedded in the fiberglass sensor body and measuring the return voltage, which can be used to infer the dielectric constant of a zone approximately 1 cm from the upper surface of the sensor (Phytos 31 manual). Using data from the PRIMET rain gauge, Tair measurements co-located with each sensor, the manufacturer recommended threshold range for when a sensor transitions from wet to dry or wet to frosted, and a simple set of logical rules, we identified distinct wetting events and classified each event at each height as wetting caused by dew, by rain, by frost, or in the cases where wetting events were likely overlapping, as wet by ambiguous source. Owing to the particular importance of the wet-to-dry threshold in the characterization of dewfall (Section 2.5), we conducted a sensitivity analysis (Supplemental S.2) and determined that a range of 270-275 mV was appropriate for capturing small dew events while avoiding misclassification of dry sensors as wet. Based on this testing a specific threshold value of 275 mV was chosen. Using an empirically derived relationship provided by the manufacturer, we interpreted wet sensor readings during each wetting event as representing < 0.1 mm depth of accumulated water or ≥ 0.1 mm depth. For more details on this conversion, as well as the decision tree for classifying wetting events, see supplemental S.3.

2.4. Seasonal boundary determination

We identified the days in each calendar year that separate the relatively rain-free dry season, when photosynthesis is limited by moisture deficit, from the relatively cold winter season, when photosynthesis is limited by low temperatures, and the relatively moist and cool shoulder seasons that separate the dry and cold periods (Emmingham and Waring, 1977; Waring and Franklin, 1979). The dry season was defined from a three-week moving average of moisture deficit/surplus, equal to daily P – PET, that was calculated moving both forward and backwards from July 15th (the midpoint of the historically driest month). The start and end of the dry season were defined as the days on which the moisture surplus/deficit indicated by the 21-day P-PET average fell below (start day) or rose above (end day) -5 mm. This threshold proved effective in isolating a continuous block of relatively rain-free days from prior and subsequent blocks of relatively rainy conditions in each of the sixteen years where the requisite data was available. In addition, the resulting start date of the dry season always fell within a period of continuously declining volumetric water content (VWC). Across the years 2005-2020, VWC at the start of the dry season ranged between 0.21 and 0.15, where field capacity at this depth is 0.25, and the observed minimum in the record was 0.06.

The start and end of the dormant cold season were then determined using a three-week moving average of $T_{air}, \ and \ a$ threshold of 5 °C. Specifically, the first time after the end of the dry season that average daily T_{air} in the moving window went below 5 °C, the last day in the moving window was marked as the starting date of the cold season. The end of the cold season was then marked as the last day in the first moving window period after the start of the following calendar year that the average crossed above the 5 °C threshold. The spring and fall shoulder

seasons were then defined as the periods between the cold and dry seasons for each year.

2.5. Predicting dry season dewfall at the canopy top

To test how accurately dewfall could be predicted during the dry season from meteorological data, we selected two approaches to classify each five-minutes interval as a period of dew accumulation or drying/surface dryness, and compared with the classified leaf wetness observations described in Section 2.3.

In the first approach, we supplied the Penman equation (Eq. (6)) with "in-tree" measurements (wind speed, RH, and Tair data from 56 m on the Discovery Tree and R_{net} data from PRIMET) and "PRIMET" measurements (all variables from the PRIMET station) to create two binary predictions based on the sign of the resulting latent heat flux (LE) estimates. In each record (in-tree vs. PRIMET), when the calculation yielded a negative LE we classified that five-minutes period as an interval of dew accumulation. All LE predictions of zero or higher were classified as nondew forming periods. We compared Penman-predicted values to observations of dew accumulation and calculated the percentage of true, false positive, and false negative predictions. This method for quantifying error is appropriate at the five-minutes time scale, but may overstate misclassification rates for applications where the exact timing of dew formation is less important than knowing whether dewfall was received on a given night or for how long. In addition, at the five-minutes scale, dewfall predictions may "flicker" from one timestep to the next as predicted LE goes just above and below 0 W m⁻². To test the Penman approach at the daily scale, we counted the number of days when it correctly predicted that dewfall occurred, and nights when it gave false positive or negative predictions. For the nights when dewfall was correctly predicted, we performed a linear regression of predicted vs. observed event length to test how well the models characterized the length of dew events.

In addition to the Penman predictions we tried a second approach, aimed at identifying the most parsimonious set of meteorological observations that could be used to predict dewfall. In this approach we examined dew-relevant predictor variables by fitting a logistic regression to each predictor individually and then to a linear combination of predictors, using observations of dewfall from the 56 m LWS (Leaf Wetness Sensor) as a binary response variable (0 = no dew accumulation, 1 = dew accumulation). In total we fit seven models each for in-tree and PRIMET observations; one for wind speed, Rnet (PRIMET only), Dewpoint depression (DPD, °C; see supplemental S.1 for calculation), relative humidity, specific humidity (SH, %) and T_{air} , in addition to a three-variable model of DPD + Wind speed + R_{net} . To make the dataset for these regressions, we pooled all observations of dew accumulation in the dry seasons of 2017–2020 (n = 1811). Non-dew data were collected between midnight and 6 a.m. on every completely dry day (no wetting registered of any type) in the dry season (n = 29,672). All regression fitting and validation was done in R version 3.6.3 using the rms package (version 6.0-1). Each logistic model was evaluated using index-corrected R² and the Area Under the Receiver Operator Curve (AUROC), a metric which quantifies the diagnostic ability of a binary classifier without requiring a specific probability threshold to be chosen. We tested the logistic model predictions at the daily scale in the same way that we tested the Penman approach at the daily scale.

3. Results and discussion

3.1. Annual wetness patterns

At the annual scale and looking only at wet vs dry periods, patterns of wetness from forest floor to canopy top were very similar – at each height, roughly half of each water year was spent wet (Table 1). Averaging all heights together, in the water years 2018–2020 the forest spent 50.2, 44.0, and 48.6% of the time wet, respectively (Table 2). These

Table 1

Percent of time that each canopy layer spends wet or dry on an annual basis and within the four seasons of the year. Statistics were calculated using all data from 2017–2020. Values represent the mean percentage across years, and values in parenthesis are one standard deviation.

Canopy layer	Annual		Cold season		Spring shoulder season		Dry season		Fall shoulder season	
	Dry	Wet	Dry	Wet	Dry	Wet	Dry	Wet	Dry	Wet
1.5 m	48.0 (6.9)	48.9 (8.3)	12.4 (11.2)	84.7 (12.7)	60.6 (9.7)	39.0 (9.4)	96.2 (4.6)	1.2 (2.3)	51.6 (15.9)	47.7 (16.4)
10 m	48.3 (3.8)	48.6 (3.5)	12.9 (7.0)	84.2 (8.4)	58.8 (7.7)	40.8 (7.7)	95.7 (4.6)	1.6 (2.8)	55.2 (4.9)	44.1 (5.2)
20 m	49.2 (3.8)	47.7 (5.5)	12.8 (9.8)	84.4 (10.1)	58.8 (9.2)	40.9 (8.9)	96.0 (4.6)	1.4 (2.6)	56.6 (6.1)	42.8 (6.3)
30 m	43.7 (3.6)	51.1 (2.6)	12.3 (8.3)	87.4 (8.2)	53.5 (3.3)	45.4 (4.0)	97.8 (2.9)	2.0 (3.1)	48.8 (11.1)	51.2 (11.1)
40 m	46.7 (5.6)	48.9 (6.9)	12.7 (7.4)	82.0 (12.5)	59.0 (9.8)	40.2 (9.9)	97.7 (2.3)	1.7 (2.6)	50.4 (12.1)	49.6 (12.1)
56 m	47.6 (3.4)	48.0 (5.2)	15.5 (7.1)	79.1 (8.7)	56.9 (6.2)	42.3 (6.3)	95.6 (1.5)	3.8 (2.1)	49.7 (8.1)	50.3 (8.1)
All layers	47.7 (4.2)	48.6 (5.2)	13.1 (7.6)	83.1 (9.8)	58.5 (7.8)	40.8 (7.7)	96.5 (2.6)	1.9 (2.4)	52.8 (8.3)	46.8 (8.6)

Table 2
Annual measures of wetting and PET derived from the summation of five-minutes observations over the course of the water years 2018, 2019 and 2020. Time spent wet presented both as an average across all height, and the length of time when any layer of the canopy was wet by a given source. Mean rainfall rate is the total depth of rainfall measured in a year, divided by the total duration of rainfall.

Year	Time spent wet (days)		Dew durati	Dew duration (days)		ng duration (days)	Rainfall duration	Mean rainfall rate	PET
	Average	Any layer	Average	Any layer	Average	Any layer	(days)	(mm hr-1)	(m)
2018	183.3	224.3	22.2	76.3	150.6	207.1	22.9	3.68	1.30
2019	160.6	205.5	23.0	73.1	121.6	176.3	20.6	3.70	1.22
2020	177.5	224.4	23.1	74.5	144.4	189.3	21.1	3.60	1.30
Mean	173.8	218.1	22.8	74.6	138.9	190.9	21.5	3.66	1.27

water years ranged from 0.56 to 1.4 standard deviations below the fifteen-year mean in annual rainfall (Fig. 3) and range from abnormally dry to severe drought conditions according to the U.S. Drought monitor (Svoboda et al., 2002), suggesting that past years in the record likely experienced higher proportions of time spent wet. Rainfall duration during the study period ranged from 20.6 to 22.9 days' equivalent a year (summed 5 min intervals with P > 0.25 mm), and the ratio of time spent rain wet to time spent raining ranged from 5.9 to 6.8 (121.5 to 155.7 days spent wet by rain). Dew wetting on average accounted for an additional 22.8 days of wetness per year, resulting in 16.4% more time spent wet than if we considered rainfall alone.

Although these annual numbers are useful for giving an idea of the wet canopy time compared to rainfall duration and amount, they mask significant seasonal variation (Fig. 4, Supplemental S.3 a-b). Averaged across all layers, the canopy was wet for an average of 83.1% of the winter, 1.9% of the dry season, and 40.8 and 46.8% of the spring and fall, respectively (Table 1).

3.2. Cold season wetness patterns

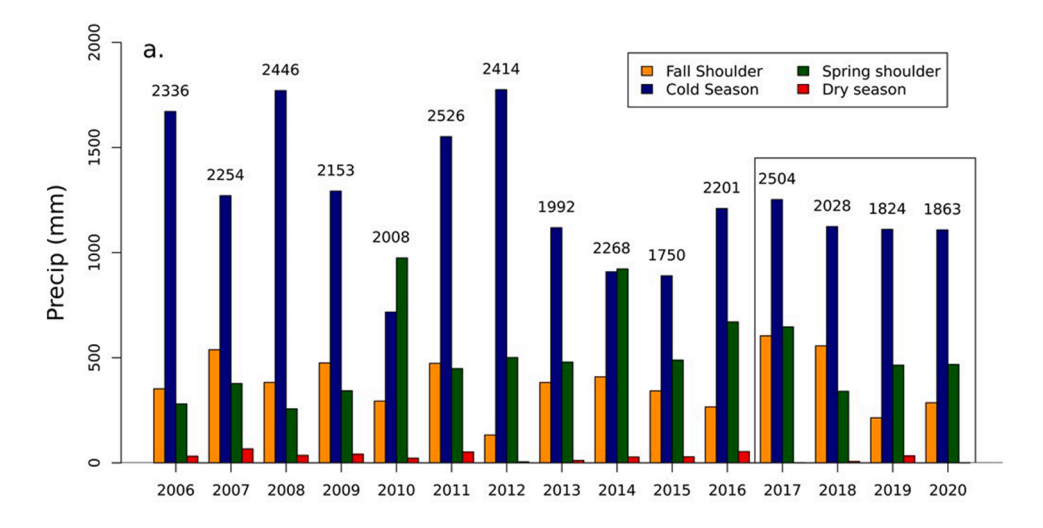
Canopy wetness varies with height during the cold season. The top canopy layer canopy spent less time wet than the forest floor (Table 1), with far more distinguishable individual wetting events and intervening dry periods (average number of events 120.8 at 56 m, 23.5 at 1.5 m, Table S.5). Dew formed on 61% of days and rain wetting was present on 68% of days at the canopy top. The relatively shorter duration wetting events in the top two canopy layers are attributable to a combination of factors related to wetting and drying - namely wind speed, air temperature, relative humidity, and incident solar radiation. Average daily wind speeds were 0.58 (SD 0.19) m $\rm s^{-1}$ at canopy top compared to 0.21 (SD 0.07) m s⁻¹ at the forest floor during the cold season, which increased the likelihood of drip from upper canopy foliage and enhanced evaporation, as did higher average daytime air temperatures (5.2 °C (SD 3.6) vs 2.9 °C (SD 2.7), top to bottom), lower average daytime RH (90.5% (SD 12.9) vs 99.4% (SD 2.4)), and more incident radiation given that shortwave radiation transmittance to the forest floor is on the order of 0.081 in forest stands of this species composition and age (Parker et al., 2002). Frost events also contributed to the pattern of high-frequency, short-duration wetting in the upper canopy and fewer, longer events lower down (Fig. 4, Table S.5a). Frost events were less frequent but lasted longer in the lower canopy, and surface drying took an order of magnitude longer than at the canopy top. Rain wetting events averaged 6.3, 7.4 and 5.9 days long in the bottom three canopy layers (Table S.5a), with one rain wetting at the 1.5m height that took 89 days to dry out. The concept of a distinct "event" breaks down below the canopy during the winter, with water likely coming from a combination of rainfall, dew deposition, and drip while taking many days to evaporate or drip dry entirely (Fig. 4). Attribution of wetness to different sources becomes challenging in lower layers of the forest in a season with such a high percentage of time spent wet.

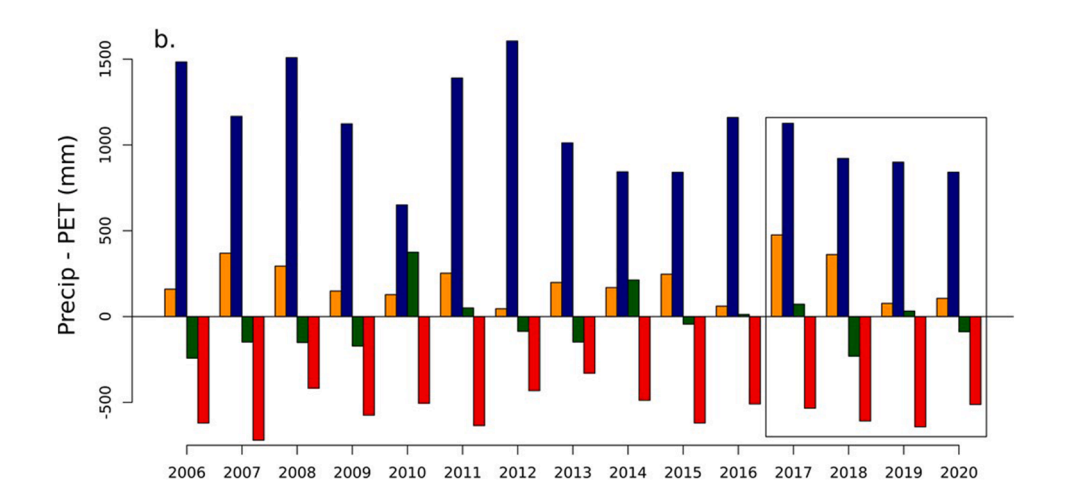
3.3. Shoulder season wetness patterns

Compared to the cold season, the shoulder seasons were relatively frost free and characterized by a less extreme version of the same pattern of higher frequency, shorter duration wetting events at the top of the canopy and longer events in the lower portions of the canopy. At the top layer of the canopy, 13.2% of dew events in spring and 46.3% in fall occurred while some part of the vertical profile was still wet from rain while the remainder occurred when all other leaf wetness sensors were dry. This suggests that water vapor originating from evaporating rain may be ventilated out of the stand more slowly after rainfall in the fall compared to spring, though eddy-covariance data and/or isotopic tracers would be needed to fully evaluate the extent to which local recycling differs between seasons (Berkelhammer et al., 2013).

Unlike the winter, each shoulder season contained dry spells, some of which lasted several weeks at heights 30m and below. Significantly more dew was observed in the fall than the spring at the top of the canopy (t-test, p=0.02), both as a percentage of time spent wet (Fig. 5) and in number of hours (Table S.5 b and d). The fifteen-year record at the PRIMET station does not show a significant difference between spring and fall in rainfall (612 vs. 584 mm, p=0.96) nor in the dewpoint depression in the two hours pre-dawn (0.17° in spring, 0.13° in fall, p=0.12). Shortwave radiation was significantly higher in the six hours after sunrise in the spring (361 W m $^{-2}$ in spring, 271 W m $^{-2}$ in fall, p<0.01) and dew events were substantially shorter in the spring than in the fall (Table S.5 b and c), suggesting enhanced evaporation in the spring compared to the fall drove differences in dewfall.

Vertical patterns in the shoulder seasons are informative with respect to the biology of poikilohydric organisms like bryophytes and lichens. In





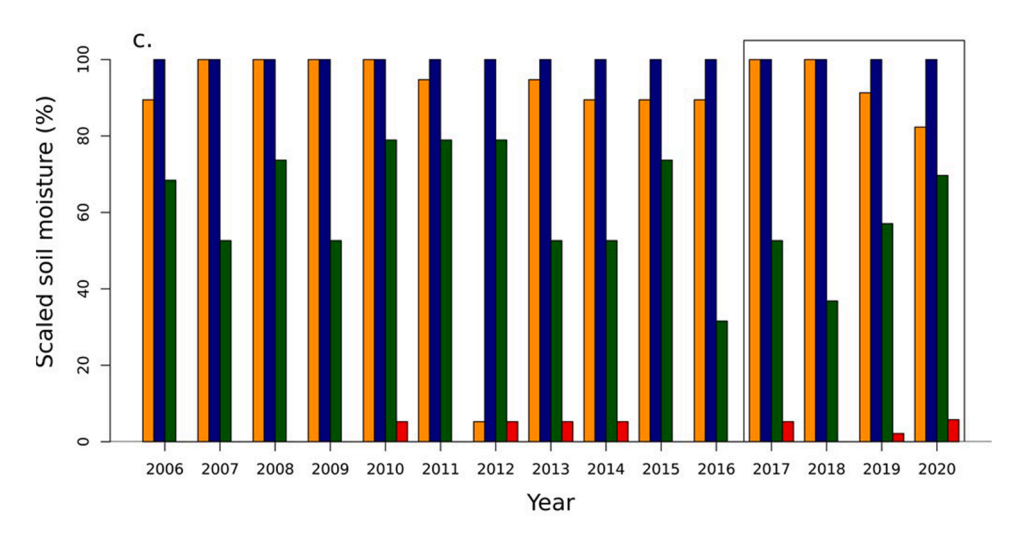


Fig. 3. Water availability in the water years 2006 to 2020, which have been divided into seasons using the methods described in Section 2.4. (a). Total rainfall values within season. Numbers above each group of bars indicate total annual rainfall in mm. (b). Total precipitation minus PET within each season. (c). remaining soil moisture at the end of each season, scaled between field capacity (0.25) and the observed minimum over the extant record (0.06).

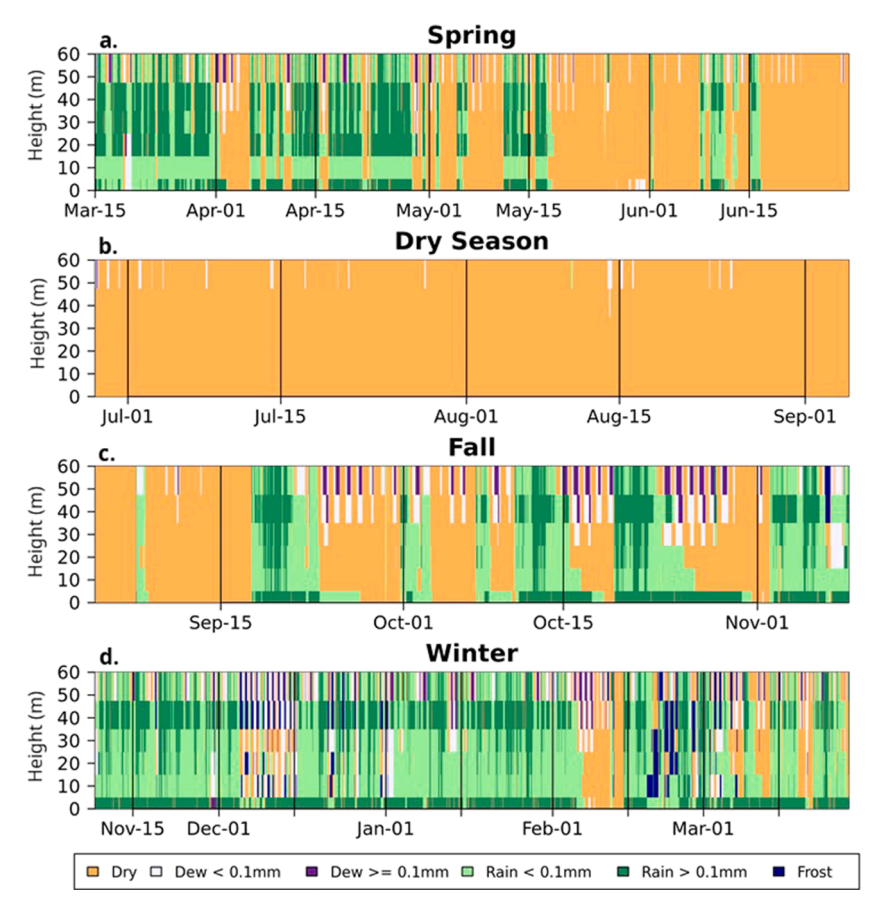


Fig. 4. Wetting by height for the (a) spring, (b) dry season, (c) fall and (d) winter seasons of the 2017 calendar year. Wetness sensors were located at 1.5, 10, 20, 30, 40 and 56 m in the canopy. Data from these sensors were converted to color bars representing intervals from 0 to 5 m, 5 to 15 m, 15 to 25 m, 25 to 35 m, 35 to 45 m, and 45 to 60 m.

general terms, wet and dry conditions were more persistent in the lower portions of the canopy, which also exhibited the longest completely dry periods. The average number of transitions from dry to wet to dry, from bottom to top were 27, 29, 28, 32, 64 and 109 in the spring and 11, 11, 12, 16, 36 and 62 in the fall. These patterns suggest that desiccationtolerant organisms living below 40 m in the canopy would go through fewer cycles of desiccation and resurrection than those living above that line. While bryophytes and lichens are capable of enduring long periods of dormancy, entering dormancy requires the costly assembly of intracellular structures that prevent damage to organelles as cells desiccate and shrink (Proctor et al., 2007). The patterns of moisture stability shown in this study are in good agreement with well-established patterns of bryophyte and lichen biomass densities with height in old growth canopies of the Pacific Northwest (McCune et al., 2000). That is, bryophyte densities are generally highest in the lower portions of the canopy, which had the fewest wet-dry transitions in this study, whereas lower densities of bryophytes and cyanobacterial lichens tend to occur in the upper canopy, which had more wet-dry transitions. Measurements of bryophyte biomass density measured on the Discovery Tree (Heffernan, 2017) also follow this pattern. This suggests that bryophytes may benefit more from longer, persistent wetting (rain, lower canopy; Csintalan et al., 2000) than from relatively short, predominantly nighttime wetting (i.e., dew, top of canopy). Moreover, in desert ecosystems where water is supplied primarily by dew, lichens sustain an overall positive carbon balance by maintaining positive net photosynthesis only during the early morning hours (Lange et al., 2006). Our work suggests that when weighing the factors that determine the distribution of epiphytic species in a given wet forest canopy, it would be fruitful to determine the carbon penalty of dormancy and resurrection for each species, as well as diurnal patterns of carbon assimilation while wet, to determine when

wetting is beneficial and when it results in a net negative carbon balance.

3.4. Wetness patterns in the dry season

In the dry season, dewfall, rather than rain, is the predominant source of canopy wetting both in frequency of events (Table S.5 d) and proportion of wetting (Fig. 5). The dry seasons of 2017 - 2020 lasted 80, 101, 98 and 76 days (Table 3). These four years were within one standard deviation of the long-term mean of 78 days (Fig. 3). Dewfall occurred on at least one canopy level on 32.5%, 26.7%, 29.6% and 25% of nights. Across years, the average duration of a dew event at the top of the canopy was 3.3 hr (SD 3.1). Dewfall was restricted primarily to the 56 m and 40 m sensor heights, which resulted in more time spent wet at the top of the canopy (3.8%, SD 2.1) than at the forest floor (1.2%, SD 2.3), a reversal of the pattern seen in all other seasons (Table 1). As noted in Section 3.3, wet and dry conditions were more persistent in the lower portions of the canopy; the average number of wet to dry transitions per dry season was 5, 8, 8, 8, 12 and 32 from the bottom to the top of the canopy.

Dew events in the dry season were shorter and had more separation from adjacent wetting than in other seasons, making it possible to look more in-depth at the timing of events and the meteorological conditions on dewy and dry nights. Dew formed at night and ranged in starting hour from shortly after sundown to briefly before sunrise (Fig. 6a). For the 70% of dew events that lasted past sunrise, some dried immediately, one event took 6 h to dry, and average time to dry was 1.4 h (SD 1.0). It should be noted that on real foliage, foliar water uptake would shorten the amount of time it takes for surface wetness to dry. In an experiment designed to determine the quantity of dew water that is taken up by

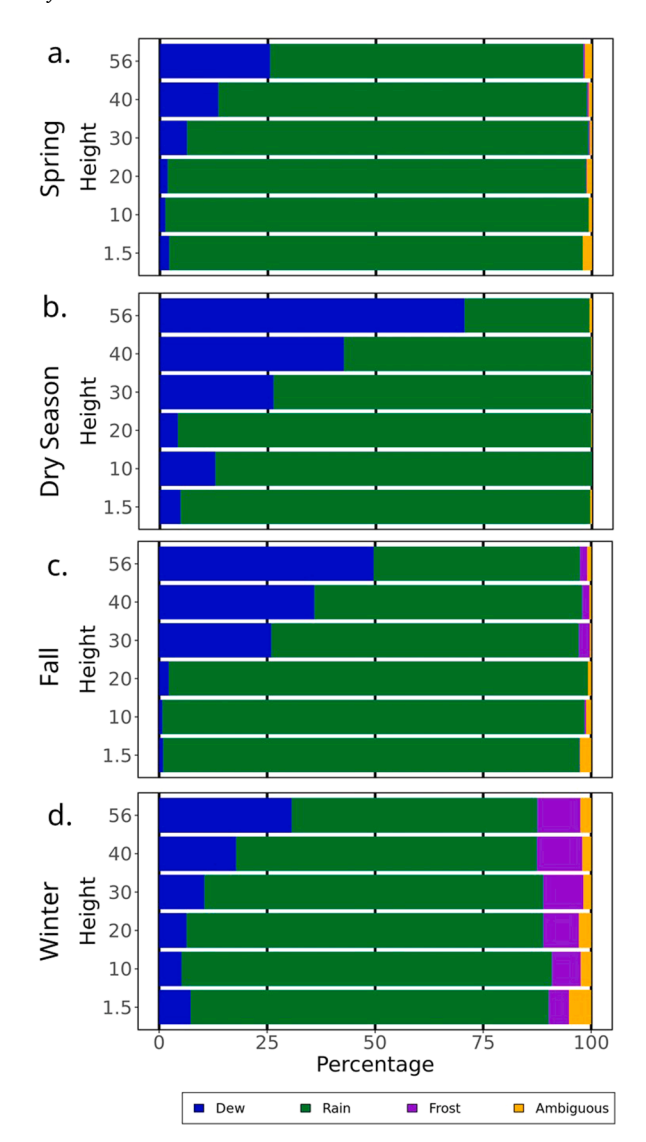


Fig. 5. Contributions to canopy wetness by type for each season across the years 2017–2020. Percentages are based on time spent wet (i.e., not the percent of time that sensors were wetted by each phenomenon, as that varied dramatically across seasons).

Table 3Seasonal boundaries for each calendar year.

Year	Spring	Dry season	Fall	Winter
2017	Mar. 15th	June 28th	Sept. 4th	Nov. 8th
2018	Mar. 27th	June 29th	Sept. 11th	Nov. 8th
2019	Mar.26th	June 9th	Sept. 8th	Nov. 2nd
2020	Mar.29th	July 4th	Sept. 15th	Nov. 1st

Douglas-fir foliage late in the summer dry season, an estimated 1.5–7.3% of water sprayed on foliage at 56 m a.g.l. in the pre-dawn hours was taken up (Sibley, 2021). This suggests that observed drying times on actual foliage may be shorter by a few percent compared to what is detected by leaf wetness sensors. Drying times of epiphytic bryophytes and lichens would also differ from that detected by the LWS due to both foliar water uptake and trapping of surface water in the intricate, three-dimensional vegetative structures of many species (Pypker et al., 2006). Enhanced retention of surface water and slow release of inter- and intra-cellular water as mosses and lichens desiccate in dry daytime conditions imply that the flux of water vapor from epiphytic bryophytes and lichens may continue for several hours after

even slight dew wetting (Pypker et al., 2017).

3.5. Dry season dewfall predictions

3.5.1. Penman model predictions

Models using the Penman equation provided better predictions of dewfall when all sensor values were obtained from the PRIMET weather station located in a canopy gap than models based on in-tree observations of Tair, RH and wind speed and PRIMET Rnet. While both methods predict dew on the overwhelming majority of true dew forming intervals (Table 4), the in-tree Penman model falsely predicts dew 1.39 times more often than there are true dew forming intervals. Increasing the value of LAI used to scale r_H would lower this false positive rate, but would come at the expense of increasing false negatives and decreasing true positives (Fig. S.2a), indicating that the in-tree sensor readings may be more responsible for the poor model performance than the parameterization of the Penman equation. The PRIMET-based model, on the other hand, can be parameterized such that false positives are greatly reduced at little expense to true positives or false negatives when LAI is raised from 1 to approximately 8 (Fig. S.2a), after which a subjective decision must be made about the desired balance between false positive and false negative predictions. While it is surprising that in-tree measurements performed more poorly than measurements at a weather station, one possible explanation is that R_{net} was only available from PRIMET, leading to a mismatch with the in-tree data. Inspection of wind data shows more variable upper-canopy wind speeds than at PRIMET, which may be another explanation for the inferior model performance using in-tree data. The more temporally variable wind speeds measured in-tree may have led to a worse representation of boundary layer conductance of the branch surface (where the LWS is located) compared to the relatively more constant nighttime winds observed at PRIMET.

The PRIMET-based Penman model parameterized with an LAI of 10 (Marshall and Waring, 1986) correctly predicted dewfall on 87% of true dew forming five-minutes intervals, with a false positive rate of 40% (Table 4). At the daily scale, 85 of the 355 summer days in the instrument record contained some dew, of which the model correctly predicted 73, with 12 false negatives and 24 false positives. On the days that dew did form, the model had a tendency to slightly overpredict the duration of the event (Fig. S.6a). This overprediction was constant across the range of true dew event lengths, and root-mean square error (RMSE) was 1.2 h. These results show that the Penman equation, when properly parameterized and driven with weather station data, can accurately capture the dynamics of dry season dewfall on a nearby canopy in a similar topographic position. However, it is unclear from the results of our study whether in-tree observations would perform less well than weather station measurements at other study sites, or if our results are caused by an issue with the in-tree sensor cluster. The results of our sensitivity analysis (Supplemental S.2) show that predictions of dew with the Penman equation are highly sensitive to the parameterization of r_H. Model fit depended on selecting an appropriate LAI value for empirical scaling by comparing Penman predictions to wetness sensor readings.

3.5.2. Logistic regression model predictions

The results of the logistic models applied to summer night data are shown in Table 5 and support the use of dewpoint depression in a parsimonious predictive model for in-tree observations. R^2 values for single variable logistic models based on either $R_{\rm net}$ or wind speed indicate the inability of these variables to explain the variance in dewfall observations, while DPD alone can explain 87% of the variance and had an AUC value of 0.994, indicating strong separation between dew and non-dew observations using in-tree DPD. The model based on RH performed similarly well, which is expected given that both DPD and RH capture the degree of saturation of the air in slightly different ways. Compared to the one-term DPD model, a three-variable model (Dew \sim DPD + $R_{\rm net}$ + Windspeed) had only a marginally better R^2 of 0.9 and an

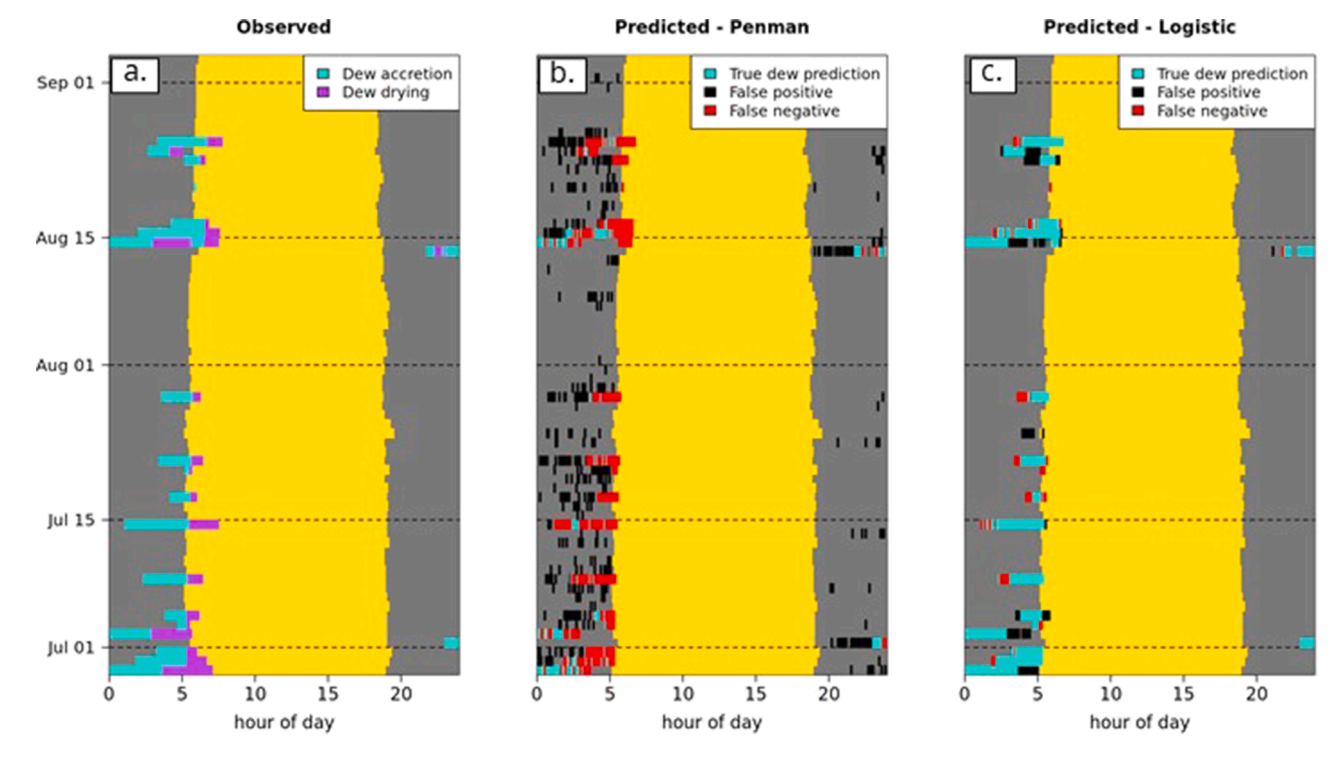


Fig. 6. Observed and predicted dew accretion and drying during the dry season of 2017. Transition between night and day denoted in all panels using gray and yellow background colors (day defined as $> 10 \text{ W m}^{-2}$ incident solar radiation). Panel a shows observed intervals of dew accretion and dew drying through the season. Panel b shows dew accretion as predicted by the Penman equation supplied with data from the PRIMET station, where LE < 0 mm is classified as a dew forming period. Panel c shows dew accretion as predicted using a logistic function with dewpoint depression as a predictor and a probability threshold of 0.5. False positives indicate where dewfall was predicted but not observed. False negatives indicate where dewfall was not predicted, but it was observed.

Table 4
Rates of false positive, false negative and correct predictions at the five-minutes scale, relative to the number of true dew accumulation events as determined by the 56 m height leaf wetness sensor, for each of the tested models. "In tree" models used data from the 56 m sensor height in the Discovery Tree, while "PRIMET" models used data from the nearby PRIMET weather station.

	In-tree		PRIMET		
	Penman	Logistic	Penman	Logistic	
False positive rate	1.39	0.233	0.4	4.62	
False negative rate	0.292	0.3	0.12	0.0068	
Correct prediction rate	0.71	0.7	0.87	0.99	

Table 5 Index corrected R^2 , AUC, intercept and slope coefficients for one-variable logistic models using data from 56 m height in the Discovery Tree.

			Coefficients		
Model	R^2	AUC	Intercept	Var	
Wind speed	0.001	0.505	-1.94	-0.11	
R _{net}	0.052	0.631	-4.26	-0.05	
Tair	0.50	0.916	5.54	-0.72	
Specific humidity	0.13	0.74	2.84	-6.84	
Relative humidity	0.87	0.994	-87.93	0.92	
DPD	0.87	0.994	4.33	-5.90	

AUC of 0.997. As the one-term DPD based model was more parsimonious we chose to show the results of applying it with a probability threshold of 0.5 to the summer of 2017 in Fig. 6c (summers of 2018–2020 in Supplemental S.4 a–c). In no case did PRIMET-based logistic models outperform the in-tree DPD model. The best one-predictor model using PRIMET data used DPD and had an $\rm R^2$ of 0.54 and AUC of 0.933. The PRIMET DPD model correctly predicted almost all true dew events, but

severely overpredicted dew (i.e., high false positive rate) when it did not occur (Table 5). The in-tree DPD model performed similarly to the PRIMET-based Penman model at both the five-minutes (Table 4) and the daily scale. At the daily scale it correctly predicting 64 out of 85 dewy days with 12 false positives and 21 false negatives at our chosen probability threshold of 0.5. The in-tree DPD model predicted the length of dew events with an RMSE of 1.1 h (Fig. S.6a).

These results indicate that the most parsimonious way to predict dewfall, in terms of instrumentation used, is to measure Tair and humidity in close proximity to the canopy of interest, which in this study was a distance of ~ 1 m. This method may also be preferable to the Penman approach for predicting differences in dewfall in different parts of a landscape. For example, at our study site, it is not obvious if the patterns of dew we observe in a valley bottom would hold for mid-slope and ridgetop topographic positions, or how PRIMET-based predictions would need to be modified to predict dew on adjacent slopes and ridges. Installing ground-based weather stations with the requisite instruments to use the Penman approach (requires Tair, RH, wind speed, and Rnet) in multiple locations across the landscape to investigate the effect of topography on dew frequency may be intractable, both from a cost perspective and in settings where forest cover is relatively unbroken and there are limited canopy openings. In such cases, outfitting multiple trees with sensors may be a more sensible approach, with the caveat that tree climbing expertise is needed.

While our study provides good evidence of the efficacy of an in-tree, dewpoint depression based logistic model for predicting dewfall, our study design did not allow us to assess the extent to which the specific parameters of our logistic model apply to other canopies across the landscape. We have recently initiated paired LWS, Tair and humidity measurements in three additional tree canopies across a range of topographic positions, which will be used to assess how widely parameters vary in different settings in a future study.

3.6. Determinants of dewfall

Examination of meteorological conditions on nights where dew did and did not form (Fig. 7) helps to explain the performance of the in-tree logistic models. Net radiation and wind speed were relatively similar in their distributions across nights where dew did and did not form, while the distributions of observed dewpoint depression at 56m were distinctly different (Fig. 7). The distribution of R_{net} values on dry nights was bimodal, with peaks at \sim -50 W m⁻² and -10 W m⁻². The latter peak likely corresponded to cloudy conditions that enhanced the local greenhouse effect and resulted in insufficient surface cooling for dew formation to occur. Outside of these relatively rare cloudy, dry season nights are the much more frequent clear nights, where there is little distinction in the distributions of R_{net} between dry and dewy nights (Fig. 7). Most dew formation happened when DPD at 56 m was < 1 $^{\circ}$ C, while DPD ranged above 12 °C on dry nights. Wind speed distributions are indistinguishable between dew and non-dew nights and largely represent still conditions ($< 1 \text{ m s}^{-1}$). Put simply, the majority of dry season nights appear to be sufficiently still and have sufficiently negative net radiation to promote cooling and dewfall, with DPD acting as the determining factor.

These results underscore the importance of dewpoint depression in determining whether dewfall occurs on a given clear-sky night in the dry season at our site. Intuitively, one would expect higher relative humidity and lower nighttime DPD after rain events and early in the season, when residual moisture from spring rains has not left the stand. While this phenomenon can be seen (Fig. 8), evidence shows that dewfall that happened more than five days since the last registered rainfall made up 61.6 % of all dew events (Fig. 8a), and 63.6 % of events happened when seasonal cumulative Precip-PET was -300 mm or lower (Fig. 7b). These numbers suggest that a large proportion of summer dewfall is driven by meteorological conditions not related to recent delivery of water, which is corroborated by the specific humidity (SH) and Tair histograms in Fig. 7 and regression results in Table 5. Specific humidity and Tair are the two determinants of dewpoint depression and viewing them independently provides a clue as to whether air cooling or an increase in specific water vapor content is responsible for DPD values < 1 °C and the subsequent occurrence of dewfall. The histograms show greater overlap in SH between dew and non-dew periods than in Tair, while the Tair logistic model yields a much higher R² and AUC than the SH model. As far as T_{air} and SH can be viewed independently, it appears that air cooling toward

the dewpoint determines when dew occurs more than an increase in SH – in fact, there is no clear evidence that SH is higher on dew nights than on non-dew nights.

The driver of enhanced air cooling in our study area is an open question and merits further investigation. Two possible drivers are cold air pooling in the valley in which the Discovery Tree stands and synoptic-scale changes in wind patterns. Cold air pooling events occur much more frequently than the formation of dewfall in the summer months in the Andrews forest (Rupp et al., 2020), meaning that the strength of the pooling and the drivers of particularly cold events would merit investigation. In the case of synoptic-scale influences, determining the drivers of dewfall would require a more complete understanding of how weather is "delivered" to the Andrews forest, which could be gained by analyzing regional scale reanalysis data. One potential determinant of dewfall may be the strength of the westerly winds, which bring relatively cooler, more humidified air to the Western cascades from above the Pacific Ocean, in contrast to Easterly winds, which bring drier, warmer, continental air masses to the forest (Taylor and Hannan, 1999; Abatzoglou et al., 2021). Given the benefit that foliar water uptake represents for water-stressed plants (Berry et al., 2018; Burgess and Dawson, 2004; Limm et al., 2009), changes in climate that are likely to decrease the frequency of dry season dew accumulation are also likely to negatively impact vegetation health. Determining the larger-scale mechanisms responsible for dry season dewfall will be important for assessing how observed and predicted changes at the regional scale will impact canopy hydration in a future where longer, hotter, and drier dry seasons are predicted (Mote et al., 2008; Salathé et al., 2008).

4. Conclusion

In this study, we observed patterns of canopy wetting in an old-growth temperate wet forest across four annual cycles. We found that canopy wetness was more persistent in the lower portions of the forest canopy in all but the dry season, and wet-to-dry transitions were less frequent in the lower than the upper canopy in all seasons. These patterns may explain the vertical distribution of poikilohydric plant and lichen biomass in the canopy of the temperate wet forests of the region. In the dry season, wetness is more frequent in the upper than lower portions of the forest canopy. Dry season wetness in the upper canopy was predominantly dewfall, which occurred on $\sim 28\%$ of nights and is a potentially important hydration source for water-stressed foliage. These

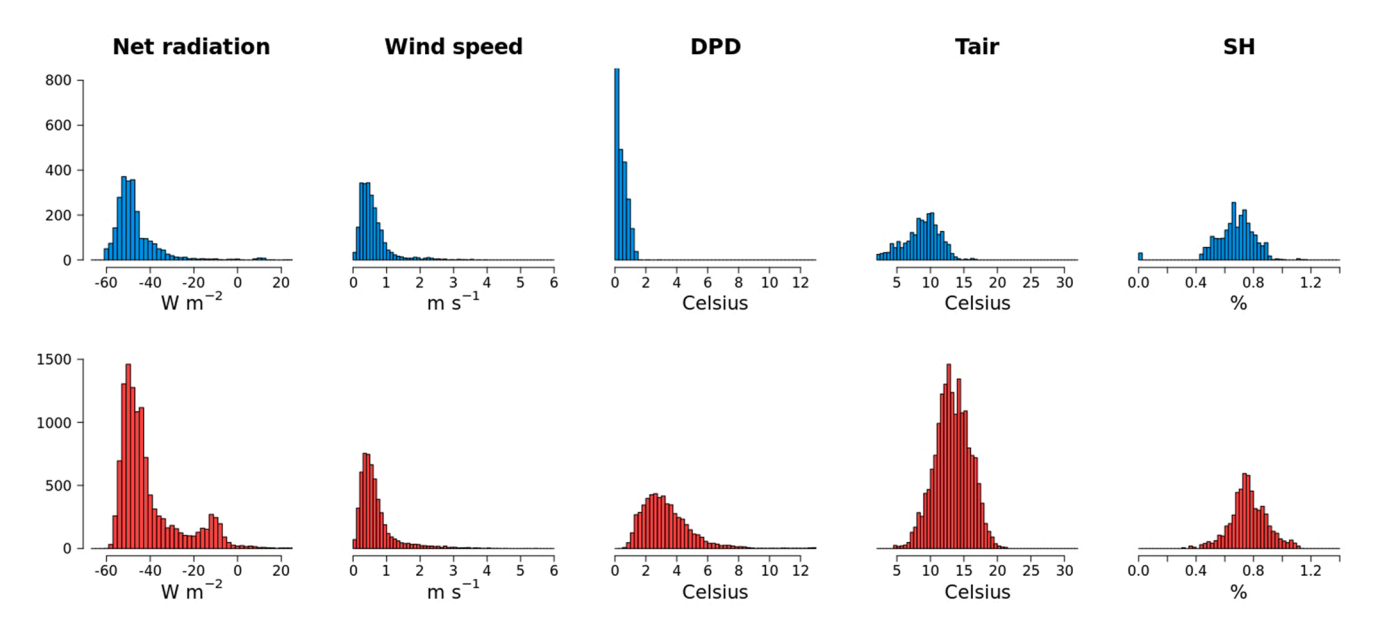


Fig. 7. Histograms of observed net radiation, wind speed, dewpoint depression (DPD), air temperature (T_{air}) and Specific Humidity (SH) during periods of dew formation (top row) and from mornings (midnight to 6am) where no dew formed (bottom row) during the dry seasons of 2017–2020.

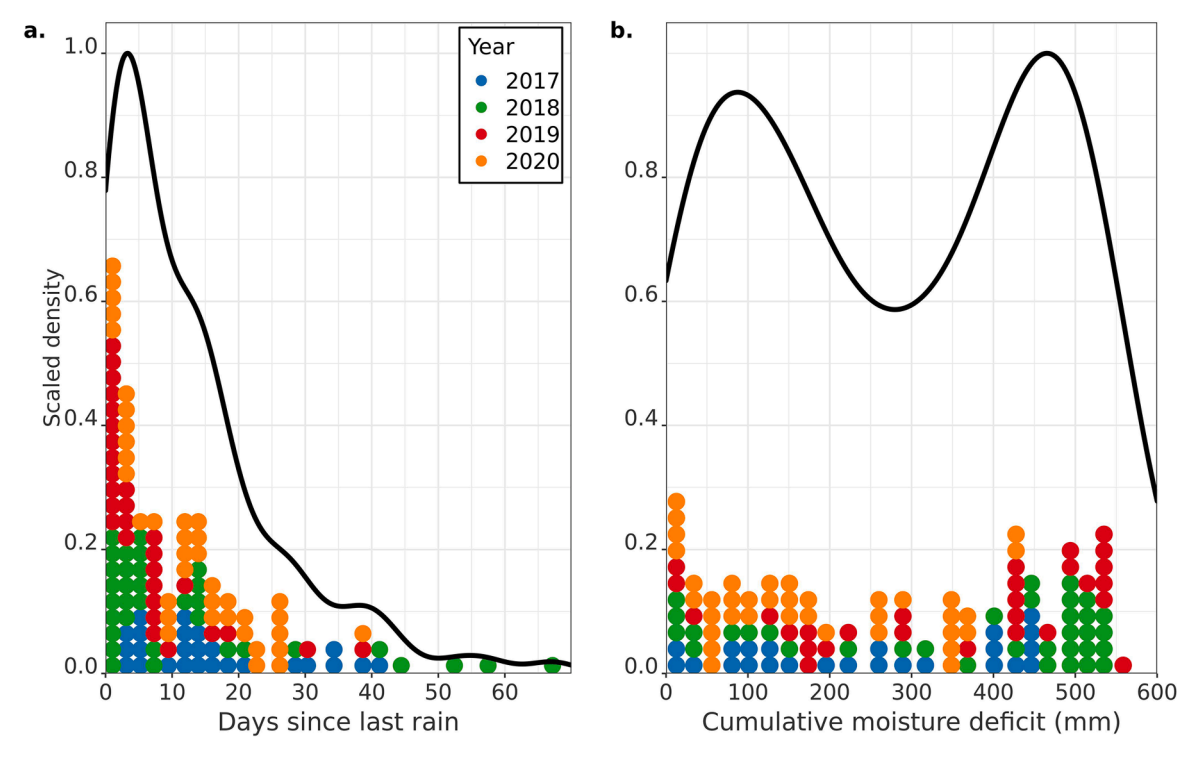


Fig. 8. Frequency of dew events relative to the number of days since the most recent rain event (a), and the cumulative moisture deficit since the beginning of the dry season (b). Filled circles along the x-axis each represent one event within a given bin, where bin sizes are 2 and 20 for panel a and b, respectively. Continuous density functions (black line) were determined by pooling all points across years and applying a Gaussian kernel density estimate.

results suggest that dew formation in temperate wet forests may be predicted using meteorological variables. In addition, because dew formation requires a dewpoint depression of $\leq 1~^{\circ}\text{C}$, ongoing increases in night-time minimum temperature may reduce dew formation in the future.

Declaration of Competing Interest

The authors declare that they have no known competing financial interests or personal relationships that could have appeared to influence the work reported in this paper.

Acknowledgments

Data and facilities were provided by the HJ Andrews Experimental Forest and the Long Term Ecological Research (LTER) program, administered cooperatively by the USDA Forest Service Pacific Northwest Research Station, Oregon State University, and the Willamette National Forest. This material is based upon work supported by the National Science Foundation under the following Grants: LTER8 DEB-2025755 (2020–2026) and LTER7 DEB-1440409 (2012–2020). Ariel Muldoon made key contributions to the statistical analysis presented in this work, and Bruce McCune gave substantial advice about bryophyte and lichen ecology and physiology.

Supplementary materials

Supplementary material associated with this article can be found, in the online version, at doi:10.1016/j.agrformet.2022.109069.

References

Abatzoglou, J.T., Rupp, D.E., O'Neill, L.W., Sadegh, M., 2021. Compound extremes drive the western oregon wildfires of September 2020. Geophys. Res. Lett. 48 (8) https:// doi.org/10.1029/2021GL092520. Andrade, J.L., 2003. Dew deposition on epiphytic bromeliad leaves: an important event in a Mexican tropical dry deciduous forest. J. Trop. Ecol. 19, 479–488. https://doi. org/10.1017/S0266467403003535.

Aparecido, L.M.T., Miller, G.R., Cahill, A.T., Moore, G.W., 2016. Comparison of tree transpiration under wet and dry canopy conditions in a Costa Rican premontane tropical forest: tropical tree transpiration response to wet and dry canopy conditions. Hydrol. Process. 30, 5000–5011. https://doi.org/10.1002/hyp.10960.

Bassimba, D.D.M., Intrigliolo, D.S., Dalla Marta, A., Orlandini, S., Vicent, A., 2017. Leaf wetness duration in irrigated citrus orchards in the Mediterranean climate conditions. Agric. For. Meteorol. 234–235, 182–195. https://doi.org/10.1016/j. agrformet.2016.12.025.

Berkelhammer, M., Hu, J., Bailey, A., Noone, D.C., Still, C.J., Barnard, H., Gochis, D., Hsiao, G.S., Rahn, T., Turnipseed, A., 2013. The nocturnal water cycle in an opencanopy forest. J. Geophys. Res. Atmos. 118 https://doi.org/10.1002/jgrd.50701, 10.225-10.242.

Berry, Z.C., Emery, N.C., Gotsch, S.G., Goldsmith, G.R., 2018. Foliar water uptake: processes, pathways, and integration into plant water budgets: foliar water uptake. Plant Cell Environ. 42, 410–423. https://doi.org/10.1111/pce.13439.

Binks, O., Finnigan, J., Coughlin, I., Disney, M., Calders, K., Burt, A., Vicari, M.B., da Costa, A.L., Mencuccini, M., Meir, P., 2021. Canopy wetness in the Eastern Amazon. Agric. For. Meteorol. 297, 108250 https://doi.org/10.1016/j. agrformet.2020.108250.

Binks, O., Mencuccini, M., Rowland, L., Costa, A.C.L., Carvalho, C.J.R., Bittencourt, P., Eller, C., Teodoro, G.S., Carvalho, E.J.M., Soza, A., Ferreira, L., Vasconcelos, S.S., Oliveira, R., Meir, P., 2019. Foliar water uptake in Amazonian trees: evidence and consequences. Glob. Chang. Biol. 25, 2678–2690. https://doi.org/10.1111/gcb.14666.

Bonan, G., 2008. Ecological Climatology: Concepts and Applications, 2nd ed. Cambridge University Press, New York, NY.

Burgess, S.S.O., Dawson, T.E., 2004. The contribution of fog to the water relations of Sequoia sempervirens (D. Don): foliar uptake and prevention of dehydration. Plant Cell Environ. 27, 1023–1034. https://doi.org/10.1111/j.1365-3040.2004.01207.x.

Campbell, G.S., Norman, J.M., 1998. An Introduction to Environmental Biophysics. Springer, New York, NY. https://doi.org/10.1007/978-1-4612-1626-1. New York.

Csintalan, Z., Takacs, Z., Proctor, M.C.F., Nagy, Z., Tuba, Z., 2000. Early morning photosynthesis of the moss Tortula ruralis following summer dew fall in a Hungarian temperate dry sandy grassland. Plant Ecol. 151, 51–54.

Daly, C., Schulze, M., McKee, W., 2019. Meteorological data from benchmark stations at the andrews experimental forest, 1957 to present. Long Term Ecol. Res. https://doi. org/10.6073/pasta/c96875918bb9c86d330a457bf4295cd9. Forest Science Data Bank, Corvallis, OR. [Database]. Available. http://andlter.forestry.oregonstate.edu/data/abstract.aspx?dbcode=MS001 (5 November 2019).

Daly, C., Smith, J.W., Smith, J.I., McKane, R.B., 2007. High-resolution spatial modeling of daily weather elements for a catchment in the Oregon Cascade Mountains, United States. J. Appl. Meteorol. Climatol. 46 (10), 1565–1586.

- Davis, K.T., Dobrowski, S.Z., Holden, Z.A., Higuera, P.E., Abatzoglou, J.T., 2019. Microclimatic buffering in forests of the future: the role of local water balance. Ecography 42, 1–11. https://doi.org/10.1111/ecog.03836.
- Dawson, T.E., Goldsmith, G.R., 2018. The value of wet leaves. New Phytol. 219, 1156–1169. https://doi.org/10.1111/nph.15307.
- De Frenne, P., Rodriguez-Sanchez, F., Coomes, D.A., Baeten, L., Verstraeten, G., et al., 2013. Microclimate moderates plant responses to macroclimate warming. Proc. Natl. Acad. Sci. 110, 18561–18565. https://doi.org/10.1073/pnas.1311190110.
- Dietz, J., Leuschner, C., Hölscher, D., Kreilein, H., 2007. Vertical patterns and duration of surface wetness in an old-growth tropical montane forest, Indonesia. Flora Morphol. Distrib. Funct. Ecol. Plants 202, 111–117. https://doi.org/10.1016/j. flora 2006.03.004
- Ehbrecht, M., Schall, P., Ammer, C., Seidel, D., 2017. Quantifying stand structural complexity and its relationship with forest management, tree species diversity and microclimate. Agric. For. Meteorol. 242, 1–9. https://doi.org/10.1016/j. agrformet.2017.04.012.
- Emmingham, W.H., Waring, R.H., 1977. An index of photosynthesis for comparing forest sites in western Oregon. Can. J. For. Res. 7, 165–174.
- Fischer, D.T., Still, C.J., Ebert, C.M., Baguskas, S.A., Park Williams, A., 2016. Fog drip maintains dry season ecological function in a California coastal pine forest. Ecosphere 7. https://doi.org/10.1002/ecs2.1364.
- Greve, P., Orlowsky, B., Mueller, B., Sheffield, J., Reichstein, M., Seneviratne, S.I., 2014. Global assessment of trends in wetting and drying over land. Nat. Geosci. 7, 716–721. https://doi.org/10.1038/ngeo2247.
- Heffernan, E., 2017. Canopy Microclimates and Epiphytes: Examining Dynamic Patterns and Influences. Oregon State University. Masters thesis. https://ir.library.oregonstate.edu/concern/graduate_thesis_or_dissertations/t722hf886?locale=en.
- Johnson, D.W., Cole, D.W., Bledsoe, C.S., et al., 1982. Nutrient cycling in forests in the Pacific Northwest. In: Edmonds, R.L. (Ed.), Analysis of Coniferous Forest Ecosystems in the Western United States. Hutchinson Ross Publishing Co., Stroudsburg, PA. US/ IBP Synthesis Ser 14Chapter 7.
- Klemm, O., Milford, C., Sutton, M.A., Spindler, G., van Putten, E., 2002. A climatology of leaf surface wetness. Theor. Appl. Climatol. 71, 107–117. https://doi.org/10.1007/ s704-002-8211-5.
- Lange, O.L., Green, T.G., Melzer, B., Meyer, A., Zellner, H., 2006. Water relations and CO₂ exchange of the terrestrial lichen *Teloschistes capensis* in the Namib fog desert: measurements during two seasons in the field and under controlled conditions. Flora Morphol. Distrib. Funct. Ecol. Plants 201 (4), 268–280. https://doi.org/10.1016/j.flora.2005.08.003 (June 2006).
- Letts, M.G., Mulligan, M., 2005. The impact of light quality and leaf wetness on photosynthesis in north-west Andean tropical montane cloud forest. J. Trop. Ecol. 21, 549–557. https://doi.org/10.1017/S0266467405002488.
- Limm, E.B., Simonin, K.A., Bothman, A.G., Dawson, T.E., 2009. Foliar water uptake: a common water acquisition strategy for plants of the redwood forest. Oecologia 161, 449–459.
- Marshall, J.D., Waring, R.H., 1986. Comparison of methods of estimating leaf-area index in old-growth Douglas-fir. Ecology 67, 975–979.
- McCune, B., 1993. Gradients in epiphyte biomass in three pseudotsuga-tsuga forests of different ages in Western Oregon and Washington. Bryologist 96, 405. https://doi. org/10.2307/3243870.
- McCune, B., Rosentreter, R., Ponzetti, J.M., Shaw, D.C., 2000. Epiphyte habitats in an old conifer forest in Western Washington, U.S.A. Bryologist 103, 417–427. https://doi.org/10.1639/0007-2745(2000)103[0417:EHIAOC]2.0.CO;2.
- McMahon, T.A., Peel, M.C., Lowe, L., Srikanthan, R., McVicar, T.R., 2013. Estimating actual, potential, reference crop and pan evaporation using standard meteorological data: a pragmatic synthesis. Hydrol. Earth Syst. Sci. 17, 1331–1363. https://doi.org/10.5194/hess-17-1331-2013.
- Meinzer, F.C., Andrade, J.L., Goldstein, G., Holbrook, N.M., Cavelier, J., Jackson, P., 1997. Control of transpiration from the upper canopy of a tropical forest: the role of stomatal, boundary layer and hydraulic architecture components. Plant Cell Environ. 20, 1242–1252. https://doi.org/10.1046/j.1365-3040.1997.d01-26.x.
- Monteith, J.L., Unsworth, M.H., 2013. Principles of Environmental Physics: Plants, Animals, and the Atmosphere, 4th ed. Elsevier/Academic Press, Boston, MA. ed.

- Mote, P., Salathé, E., Dulière, V., Jump, E., 2008. Scenarios of Future Climate for the Pacific Northwest. University of Washington, WA. Report of the Climate Impacts
- Parker, G.G., Davis, M.M., Chapotin, S.M., 2002. Canopy light transmittance in Douglasfir-western hemlock stands. Tree Physiol. 22, 147–157. https://doi.org/10.1093/ treephys/22.2-3.147.
- Pincebourde, S., Casas, J., 2015. Warming tolerance across insect ontogeny: influence of joint shifts in microclimates and thermal limits. Ecology 96, 986–997. https://doi. org/10.1890/14-0744.1.
- Proctor, M.C.F., Oliver, M.J., Wood, A.J., Alpert, P., Stark, L.R., Cleavitt, N.L., Mishler, B. D., 2007. Desiccation-tolerance in bryophytes: a review. Bryologist 110, 595–621. https://doi.org/10.1639/0007-2745(2007)110[595:DIBAR]2.0.CO;2.
- Pypker, T.G., Unsworth, M.H., Bond, B.J., 2006. The role of epiphytes in rainfall interception by forests in the Pacific Northwest. II. Field measurements at the branch and canopy scale. Can. J. For. Res. 36, 819–832.
- Pypker, T.G., Unsworth, M.H., Van Stan, J.T., Bond, B.J., 2017. The absorption and evaporation of water vapor by epiphytes in an old-growth Douglas-fir forest during the seasonal summer dry season: implications for the canopy energy budget: impact of epiphytes on the canopy hydrology of Douglas-fir forests. Ecohydrology 10, e1801. https://doi.org/10.1002/eco.1801.
- Ritter, F., Berkelhammer, M., Beysens, D., 2019. Dew frequency across the US from a network of *in situ* radiometers. Hydrol. Earth Syst. Sci. 20, 1179–1197.
- Rothacher, J., Dyrness, C.T., Fredriksen, R.L., 1967. Hydrologic and Related Characteristics of Three Small Watersheds in the Oregon Cascades. Pacific Northwest Forest and Range Experiment Station Publication, Portland, OR.
- Rupp, D.E., Shafer, S.L., Daly, C., Jones, J.A., Frey, S.J.K., 2020. Temperature gradients and inversions in a forested cascade range basin: synoptic- to local-scale controls. J. Geophys. Res. Atmos. 125 https://doi.org/10.1029/2020JD032686.
- Salathé, E.P., Steed, R., Mass, C.F., Zahn, P.H., 2008. A high-resolution climate model for the U.S. pacific northwest: mesoscale feedbacks and local responses to climate change. J. Clim. 21, 5708–5726. https://doi.org/10.1175/2008JCLI2090.1.
- Schmitz, H.F., Grant, R.H., 2009. Precipitation and dew in a soybean canopy: spatial variations in leaf wetness and implications for *Phakopsora pachyrhizi* infection. Agric. For. Meteorol. 149, 1621–1627. https://doi.org/10.1016/j.agrformet.2009.05.001.
- Sentelhas, P.C., Gillespie, T.J., Batzer, J.C., Gleason, M.L., Monteiro, J.E.B.A., Pezzopane, J.R.M., Pedro, M.J., 2005. Spatial variability of leaf wetness duration in different crop canopies. Int. J. Biometeorol. 49, 363–370. https://doi.org/10.1007/ s00484-005-0250-1
- Priestley, C.H.B., Taylor, R.J., 1972. On the Assessment of Surface Heat Flux and Evaporation Using Large-Scale Parameters. Monthly Weather Review 100, 81-92.
- Sibley, A., 2021. Plants and Their Environment: Assessing Canopy Microclimate and the Response of Trees to Environmental Stress in a Diversity of Forest Types. Oregon State University. Doctoral dissertation. https://ir.library.oregonstate.edu/concern/graduate_thesis_or_dissertations/gq67jz82j.
- Storlie, C., Merino-Viteri, A., Phillips, B., VanDerWal, J., Welbergen, J., Williams, S., 2014. Stepping inside the niche: microclimate data are critical for accurate assessment of species' vulnerability to climate change. Biol. Lett. 10, 20140576 https://doi.org/10.1098/rsbl.2014.0576.
- Svoboda, M., LeComte, D., Hayes, M., Heim, R., Gleason, K., Angel, J., Rippey, B., et al., 2002. The drought monitor. Bull. Am. Meteorol. Soc. 83 (8), 1181–1190.
- Swanson, F.J., James, M.E. 1975. Geology and geomorphology of the H.J. Andrews experimental forest, western Cascades, Oregon. Research Paper PNW-188. U.S. Department of Agriculture, Forest Service, Portland, OR., 1 14.
- Taylor, GH, Hannan, C., 1999. The Climate of Oregon: From Rain Forest to Desert. Oregon State University Press, Corvallis, OR.
- Van Pelt, R., North, M.P., 1996. Analyzing Canopy structure in pacific northwest oldgrowth forests with a stand-scale crown model. Northwest Sci. 70, 15–30.
- von Arx, G., Graf Pannatier, E., Thimonier, A., Rebetez, M., 2013. Microclimate in forests with varying leaf area index and soil moisture: potential implications for seedling establishment in a changing climate. J. Ecol. 101, 1201–1213. https://doi.org/ 10.1111/1365-2745.12121.
- Waring, R.H., Franklin, J.F., 1979. Evergreen coniferous forests of the pacific northwest. Science 204, 1380–1386.